Kernel-Phase Interferometry for Super-Resolution Detection of Faint Companions

Samuel M. Factor, Adam Kraus
Dept. of Astronomy, The University of Texas at Austin

The University of Texas at Austin

Contact Information
Website: smfactor.github.io
Email: sfactor@astro.as.utexas.edu

S. Factor is P.I. of HST Cycle 24 Archival project 14561 which is supporting this work.

Kernel-phases are self calibrating observables used for high contrast imaging **at or even below λ/D**. We are currently using this technique to search for companions to nearby brown dwarfs in archival HST images. The pipeline will be particularly **applicable to JWST** and the future 30m class telescopes and will be **available soon as a python package**.

Background

The detection of companions to stars—both planets and stellar binaries—has traditionally relied on three methods: radial velocities (RVs), transits/eclipses, and direct imaging.

- Transit and RV surveys are insensitive to companions at large semimajor axes. While direct-imaging surveys are more sensitive to such objects, **there is often a gap inside the inner working angle of direct imaging and outside the regime where transits and RVs can efficiently survey.**
- Imperfections in the optical path (and AO correction) introduce "speckles" which can be misinterpreted as companions. Speckles can be corrected using many different techniques but all tend to fail near λ/D.
- Interferometric analysis takes advantage of the wave nature of light and can be used to reject speckle noise and detect companions with high contrast *at or even below* the diffraction limit. **Rather than subtracting off the PSF, these techniques uses the information contained in it to infer the geometry of the source.** The discovery of the newly forming giant planet LkCa15 b by Kraus & Ireland (2012) demonstrates the power of such techniques (see Fig. 1).

Filling the gap between RV and transit surveys and classical direct imaging surveys would offer a crucial new view of both exoplanetary systems and stellar multiplicity.

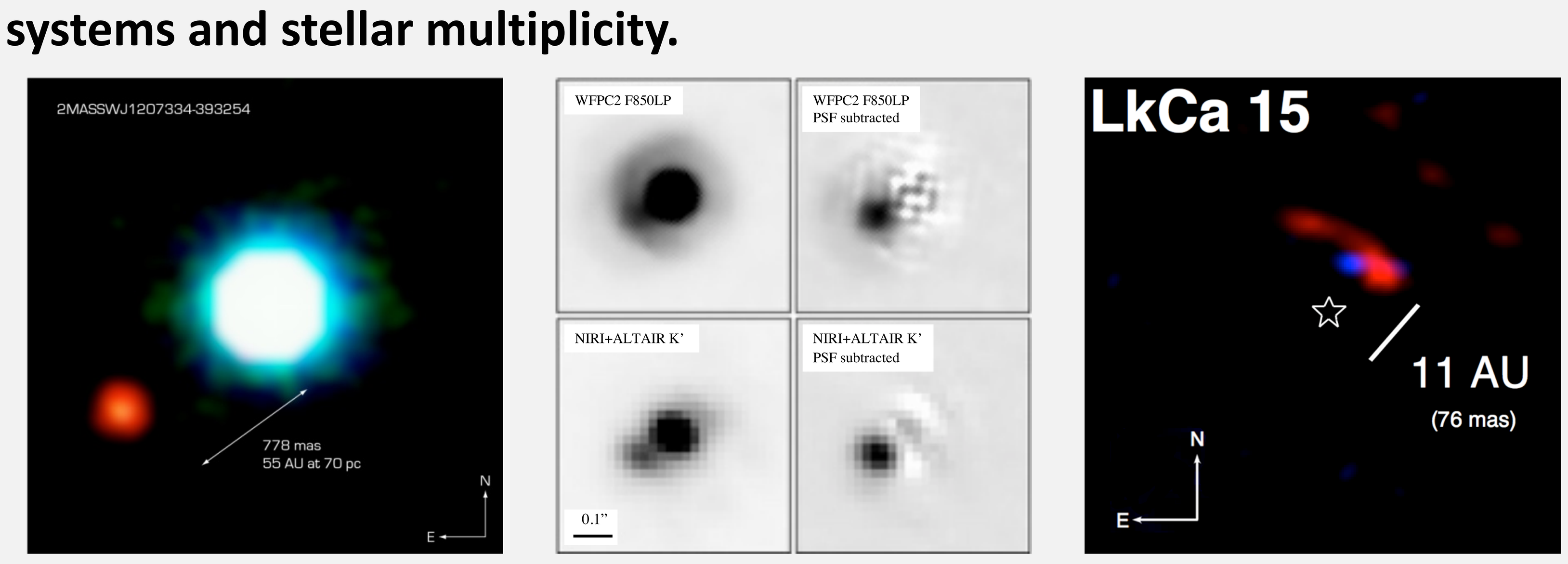

Figure 1: Examples of previously imaged low-mass companions. *Left*: VLT NACO image of 2MASS 1207 AB, a brown dwarf with a ~7 M_{Jup} companion at ~55 au (Chauvin et al. 2004). *Center*: WFPC2 and NIRI+ALTAIR raw and PSF subtracted images of the young brown dwarf 2MASS J044144 with a 5-10 M_{Jup} companion at 15 au (Todorov et al. 2010). *Right*: Keck NRM K' (blue) and L' (red) band reconstructed images of LkCa 15 b, a ~6 M_{Jup} companion at ~20 au inside the gap of a transitional disk around a ~2 Myr old solar analogue (Kraus & Ireland 2012).

Results: A widely applicable pipeline for high contrast imaging at λ/D

Fig. 3 and 4 show a marginally resolved binary brown dwarf observed by Reid et al. (2006) and an unresolved binary observed by Pravdo et al. (2004) (and reanalyzed by Martinache 2010). We are currently analyzing a large set of HST NICMOS/NIC1 observations to search for close in binary and triple brown dwarf systems. **We fit and statistically compare single and double point models using Bayesian model comparison** (using `PyMultiNest`; Buchner et al. 2014). Previous estimates of the detection limits (Martinache 2010, Pope et al. 2013) show a detection with **50:1 contrast at 80 mas (0.5λ/d at 1.9 μm) or 3:1 contrast at 35 mas** is possible with 99% confidence. In Taurus, these correspond to a few M_{Jup} mass planet at 10 au around a late M or brown dwarf or a similar mass binary at 5 au. We are currently measuring our pipeline's detection limits.

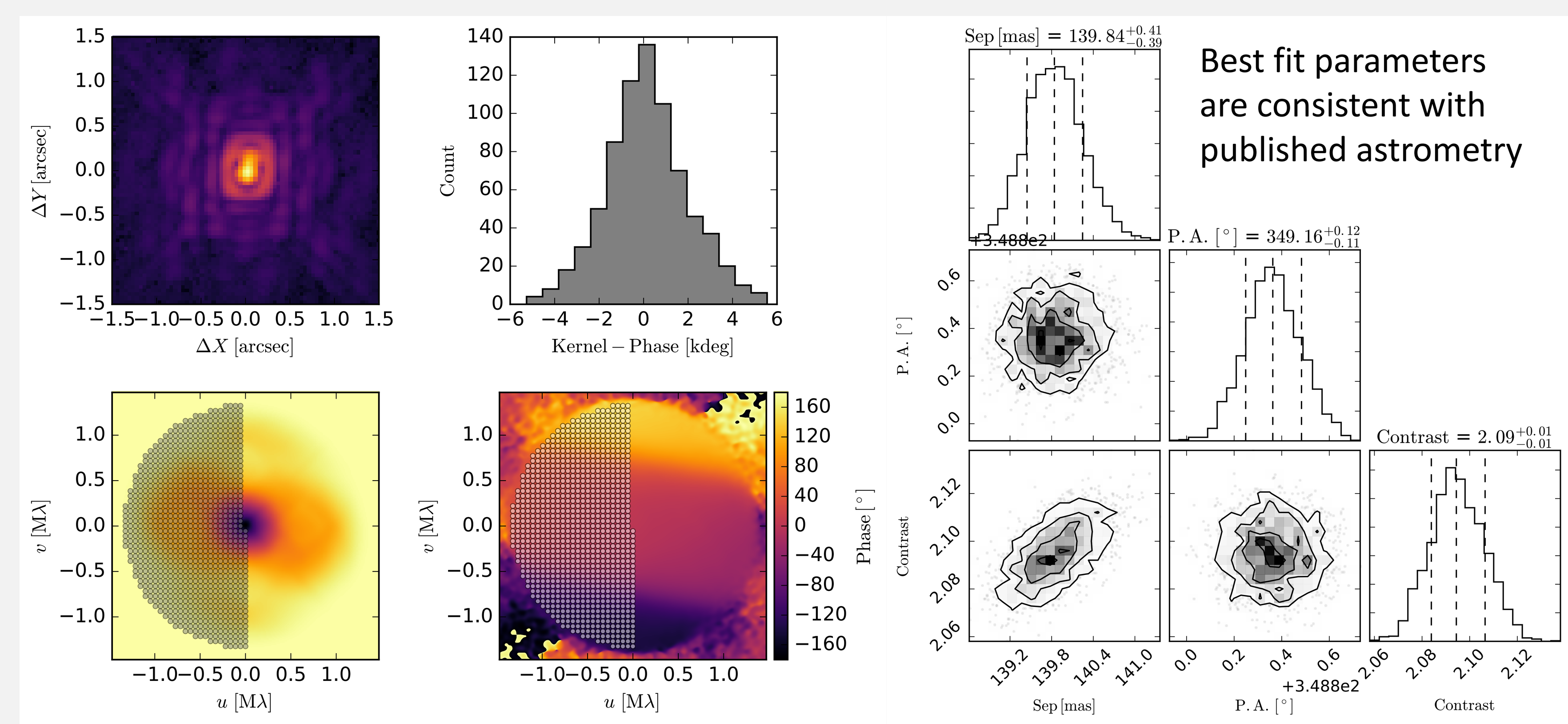

Figure 3: *Left*: The progression from image to kernel-phase. *Counter-clock-wise from the top left*: HST NICMOS1 image of 2MASS J014732 (F170M, Reid et al. 2006), Fourier amplitude, Fourier phase, and kernel-phases calculated from the sampled phases. Grey circles show the sampled points. A single point would have kernel-phases of 0° (with some small spread). *Right*: corner plot showing the 1- and 2D posteriors of fitting 3-parameter double point source model to the kernel-phases to the right.

Figure 4: Results of fitting a simple double point source model to the HST NICMOS1 image of GL 164 in the lower right (F190N , up is at a PA of 208°). *Left*: Corner plot showing the 1- and 2D posteriors of the three parameter fit. *Top Right*: Kernel-phases generated from the image (using SAO 179809 as a calibrator) plotted against those from the best fit model. A 1-to-1 correlation, shown by the green line, indicates a good fit.

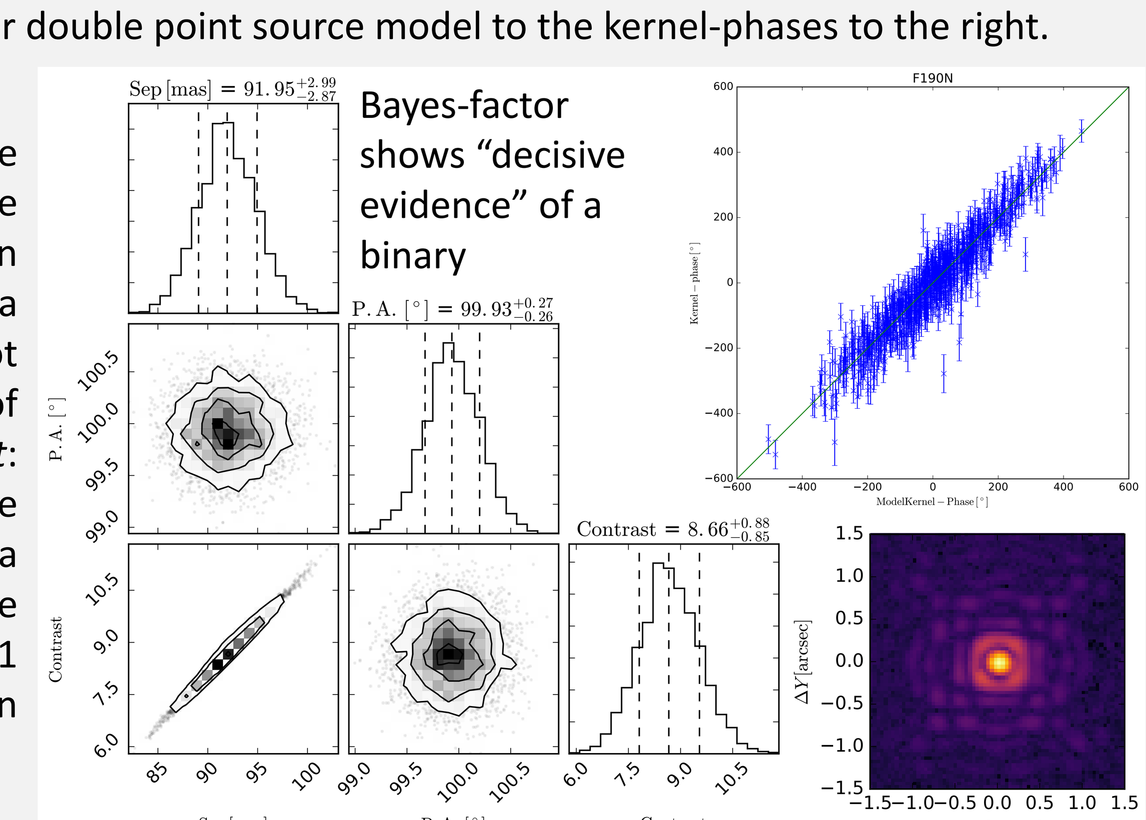

What is a Kernel-Phase?

Non-redundant masking (NRM), the most common interferometric technique for single-aperture telescopes, places a mask in the pupil plane, transforming a large single aperture into a sparse interferometer. This mask only allows ~5% of the light to reach the detector, imposing a *severe* flux limit. **Kernel-phase analysis models the *full aperture* as a grid of sub-apertures** (Fig. 2). This defines which spatial frequencies are sampled. We examine the *phase* of the Fourier transform of the image to infer the source geometry.

Each pair of apertures, or baselines, contributes both the true phase of the source and a phase error from each of the apertures. Combining all the baselines together, we can write a matrix equation for the measured phases:

$$\Phi = \Phi_o + \mathbf{A}\cdot\phi \qquad (1)$$

Where Φ is a vector of the measured phases from each baseline, Φ_0 is the true source phase, **A** is a matrix encoding which apertures contribute to each baseline, and ϕ is a vector of the phase errors from each aperture. Each column of **A** corresponds to an aperture while each row corresponds to a baseline.

To derive an equation which is independent of the phase errors we use singular value decomposition to calculate the kernel (**K**) of **A** such that

$$\mathbf{K}\cdot\mathbf{A} = 0 \qquad (2)$$

We can then multiply both sides of Equation 1 by **K** to get

$$\mathbf{K}\cdot\Phi = \mathbf{K}\cdot\Phi_o + \mathbf{K}\cdot\mathbf{A}\cdot\phi$$
$$= \mathbf{K}\cdot\Phi_o \qquad (3)$$

This produces observables called kernel-phases (first presented by Martinache 2010) which are independent of phase errors, similar to closure-phases used with NRM. **This technique can achieve similar detection limits to NRM in a fraction of the time and can be applied to dimmer sources where NRM is not feasible, as well as archival data sets.**

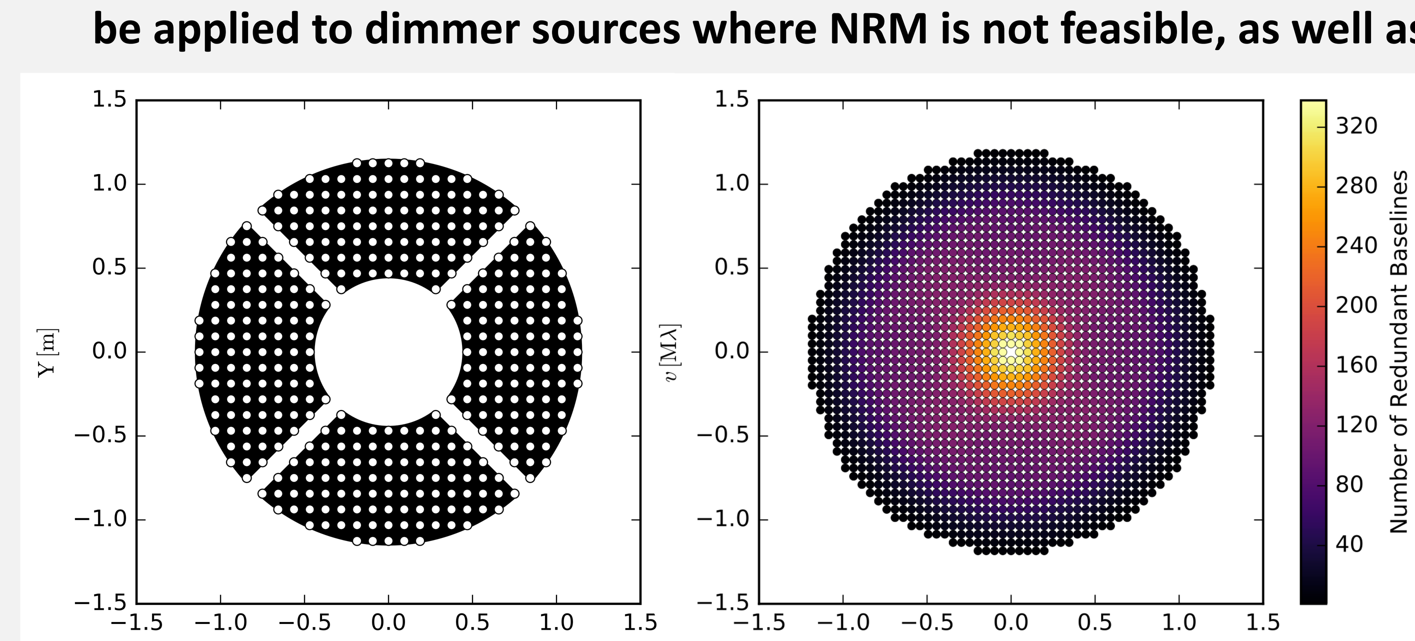

Figure 2: *Left*: Model HST aperture. *Right*: The corresponding baselines (at 1.9 μm), color-coded by the number of distinct pairs of subapertures which contribute to the point. The 392 sub-apertures sample 938 unique baselines and generate 745 kernel-phases.